Vol. 1: 63–75, 2007
doi: 10.3354/ab00006

AQUATIC BIOLOGY
Aquat Biol

Printed October 2007
Published online September 18, 2007

OPEN ACCESS

Dispersal of sea louse larvae from salmon farms: modelling the influence of environmental conditions and larval behaviour

Philip A. Gillibrand[1,*], Kate J. Willis[1]

[1]**Scottish Association for Marine Science, Oban, Argyll PA37 1QA, UK**

ABSTRACT: Sea lice are ectoparasitic copepods of farmed and wild salmonids that cost the global salmon aquaculture industry more than US $100 million annually and have been implicated as a contributing factor in the decline of wild salmonid populations in the North Atlantic region. A coupled hydrodynamics–louse-transport model including varying physical forcing and sea louse larval behaviour was developed, and used to investigate: (1) the dispersal of sea louse larvae from a point source in an idealized coastal inlet; (2) the effect of physical processes on louse distributions; and (3) the effect of behavioural processes on louse distributions. The dispersal and distribution of sea louse larvae was strongly influenced by environmental conditions and larval behaviour. In particular, larval diel vertical migration increased the predicted infection risk for wild salmonids, as more sea louse larvae were retained within the inlet and were dispersed more widely with higher average abundance at the surface. When wind forcing was weak or channelled along the inlet, higher louse abundance was predicted along the boundaries, where migrating salmonids tend to congregate. Copepodids were intermittently transported to the river mouth at the head of the inlet during different combinations of river flow and wind forcing, either by surface flows or deeper landward-flowing currents. Mean predicted nauplius abundance peaked near the source of larvae and decreased rapidly with increasing distance from the source, whereas copepodids peaked 7 to 12 km seaward of the source. Realistic environmental forcing and larval behaviour must be incorporated into dispersal models if the spatial and temporal variability of larval sea louse abundance is to be reliably predicted.

KEY WORDS: *Lepeophtheirus salmonis* · Salmon aquaculture · Particle tracking model · Hydrodynamic model · Larval transport · Infective risk · Diel vertical migration · Salmonids

INTRODUCTION

Sea lice are ectoparasitic copepods that graze on the skin and mucus of salmonids resulting in lesions, osmoregulatory problems, and secondary infections that can cause severe problems in both wild and farmed salmon (Pike & Wadsworth 2000, Costello 2006). In the northern hemisphere, *Lepeophtheirus salmonis* is the most common species of sea louse, and is responsible for serious disease problems on farmed Atlantic salmon (Pike & Wadsworth 2000, Costello 2006). The global cost of sea lice to the salmon aquaculture industry due to indirect and direct losses is estimated to be greater than US $100 million annually (Johnson et al. 2004).

Dwindling numbers of wild salmonids in farming areas have been attributed to the expanding aquaculture industry and the increased prevalence of sea louse infestations on salmon farms (Tully & Whelan 1993, Northcott & Walker 1996). In 2004, approximately 800 000 t of salmon were farmed in the North Atlantic (ICES 2005). This high biomass of salmon confined to cages provides an abundant supply of hosts for sea lice, augmenting planktonic louse populations in inshore

*Email: philip.gillibrand@sams.ac.uk

waters (Tully & Whelan 1993, Heuch & Mo 2001, Butler 2002). Tully & Whelan (1993) suggested that 95% of larval sea lice originate from farmed salmon in some areas along the west coast of Ireland, while Butler (2002) concluded that in Scottish waters less than 1% originated from wild salmonids. Thus, farmed salmon are likely to be a major source of the sea lice that infect migrating wild salmonids, potentially reducing their survival (Tully & Whelan 1993, Tully et al. 1999, Bjorn et al. 2001, Bjorn & Finstad 2002), and causing the fish to return prematurely to freshwater in some regions (Birkeland & Jakobsen 1997, Bjorn et al. 2001).

The sea louse *Lepeophtheirus salmonis* has 3 free-swimming planktonic larval stages: 2 nauplii and an infective copepodid. These non-feeding larval stages rely on yolk reserves to survive, and drift with the prevailing current until the copepodid encounters a host fish to attach to, whereupon it begins feeding and development progresses through a further 7 stages on the host. Until recently, larval sea lice were only found consistently within, or close to, salmon cages, and sporadically in the vicinity of river mouths (Costelloe et al. 1998a,b). The inverse relationship between the distance from salmon farms and larval abundance led Costelloe et al. (1998a,b) to conclude that sea lice were retained within the farm cages, and that wild salmon and sea trout were the sources of lice found at river mouths, as opposed to dispersal of larvae from fish farms. This conclusion is now being questioned with Penston et al.'s (2004) finding of both nauplii and copepodids in open water in Loch Shieldaig, Scotland, distant from the nearest salmon farm. The biannual cycle of louse abundance along the shoreline at the head of Loch Shieldaig matched the production cycle of the local salmon farms, with the appearance of louse copepodids lagging behind farm louse burdens by 1 to 3 wk (McKibben & Hay 2004).

In parallel with the studies of Penston et al. (2004) and McKibben & Hay (2004), a particle transport model was developed to simulate louse dispersal in Loch Shieldaig (Murray & Gillibrand 2006). Modelled results demonstrated that viable louse larvae could be transported many kilometres from their source and dispersed throughout the sea loch, with lice aggregations occurring at the head of the loch under certain wind conditions, thus supporting the field observations. The widespread dispersal and wind-driven aggregations of lice also suggested that wild salmonids could encounter elevated densities of infective lice during their seaward migrations.

The model described by Murray & Gillibrand (2006) assumed that sea lice are buoyant, and consequently larval dispersal was very dependent on wind-driven surface currents. The importance of wind-, tidal- and freshwater-driven currents and larval development time in determining the spatial distribution of sea louse larval stages is well recognised, and larval behaviour is also likely to influence dispersal patterns. Murray & Gillibrand's (2006) model (as well as other models of lice dispersal e.g. Asplin et al. 2004, Brooks & Stucchi 2005, Krkošek et al. 2005) did not include all the key physical and hydrodynamic parameters, and no previous sea louse modelling studies have included louse behaviour such as diel vertical migration (DVM) or aggregation at haloclines. Without the development of models incorporating these key processes, accurate prediction of lice dispersal and zones of infection — and therefore management of coastal zones with regard to farm location and transfer of sea lice to wild salmonids — will remain difficult. In this paper, we describe the development and use of a coupled hydrodynamic–louse transport model to investigate the influence of physical forcing and larval behaviour on the dispersal of sea louse larvae from a point source in an idealized coastal inlet. The model includes key hydrodynamic and sea louse behaviour processes: wind, freshwater runoff, tidal currents, temperature-dependent growth, mortality, salinity preference, and DVM. To our knowledge, this is the first model study to couple larval louse behaviour with 3D circulation, a research gap noted by Costello (2006).

METHODS

Dispersal of larvae of the sea louse *Lepeophtheirus salmonis* was modelled using 'meta-particles', each of which represented a cohort of larvae. The particle tracking sub-model was embedded within the hydrodynamic model, and was applied to an idealized coastal inlet; the use of an idealized domain permitted investigation of generic, system-independent, aspects of larval dispersal.

Hydrodynamic model. The hydrodynamic model has been described previously (e.g. Saucier et al. 2003) and a recent application of the model to a Scottish inlet is described by Gillibrand & Amundrud (2007). The model is a 3D free-surface z-coordinate primitive-equation model (with Boussinesq and hydrostatic approximations). The prognostic variables are water level (η), water temperature (T), salinity (S) and the 3 components of velocity u, v, w along the horizontal axes x and y and vertical axis z (positive upward). Discretisation is by finite-differences on an Arakawa C-grid. A 2 time-level scheme is used, and the prognostic variables are stepped forward in time, from a specified initial state, with a time step of 30 s. Horizontal viscosity (A_H) and diffusion (K_H) are parameterized using the Smagorinsky algorithm with a constant of $\alpha = 0.2$.

Coefficients of vertical viscosity and diffusion (A_V, K_V) were derived using a Mellor-Yamada level 2.2

turbulence-closure scheme (Simpson et al. 1996), whereby the temporal evolution of turbulent kinetic energy (TKE) is determined by the balance between production, dissipation and vertical diffusion of TKE. The vertical diffusion coefficient, K_V, was utilised in the random walk element of the particle transport model, as described below.

The idealized domain (Fig. 1) is a rectangular basin, orientated east to west, and of length 30 km, width 2 km, and depth 40 m (typical dimensions of a mid-size Scottish inlet). At a distance of 20 km from the open mouth of the domain, the channel narrows and shoals to 1 km width and 20 m depth, representing a silled constriction such as are commonly found in fjords. The inlet is also tapered slightly towards the head where the river discharges. The domain is represented by a Cartesian grid with a horizontal resolution of 100 m and a vertical resolution of 4 m. This relatively coarse vertical resolution is required so that the surface grid layer can accommodate a tidal oscillation of amplitude 1.5 m (see 'Methods — Experimental setup'); however, as a result of this coarse vertical resolution, wind-driven currents, which are strongest at the surface, and, to a lesser extent density-driven currents, may not be fully resolved. In the idealized scenarios presented here, where the wind forcing is oscillatory, the error incurred is unlikely to be substantial. In future simulations, where real wind forcing is used for real site studies, it will be important to ensure that the hydrodynamic model fully resolves the vertical profiles of the wind- and density-driven circulation.

The model was forced by sea-surface height at the inlet mouth ($x = 0$), spatially-uniform wind stress at the surface, and freshwater input at the head of the inlet. At the open boundary, depth-independent values of $S = 34.2$ and $T = 10$°C were specified. Treatment of the prognostic variables at the open boundary is described by Gillibrand & Amundrud (2007). Both the wind forcing and river discharge are able to vary temporally, but for these simulations the river flow was held constant during each run.

Particle transport model. The particle tracking model is embedded within the hydrodynamic model and is able, therefore, to utilise the most recent values of temperature, salinity and velocity without any temporal interpolation. The 3D location of a particle at time t, X_p^t (x,y,z), is calculated according to

$$X_p^t(x,y,z) = X_p^{t-\Delta t}(x,y,z) + \Delta t.\left[U_p(x,y,z) + w_p(z)\right] + \delta_H(x,y) + \delta_Z(z) \quad (1)$$

where Δt is the time step of the particle tracking algorithm, $U_p(x,y,z)$ is the 3D model velocity at the particle location, $\delta_H(x,y)$ and $\delta_Z(z)$ represent horizontal and vertical eddy diffusion respectively, and $w_p(z)$ represents the vertical swimming speed. Particle advection is treated using a 4th-order Runge-Kutta algorithm.

Horizontal and vertical eddy diffusion is represented in the model by the 'random walk' displacement terms $\delta_H(x,y)$ and $\delta_Z(z)$ respectively. The horizontal term is given by:

$$\delta_H(x,y) = \gamma[6.K_H.\Delta t]^{1/2} \quad (2)$$

where γ is a real random number ($\gamma \in [-1, 1]$) and K_H is the horizontal eddy diffusivity. For the present simulations, we use a small constant eddy diffusivity of $K_H = 0.1$ m^2 s^{-1}. Vertical eddy diffusion is treated by specifying

$$\delta_Z(z) = \gamma\left[6.K_V(z_p^\star).\Delta t\right]^{1/2} + K'_V(z_p).\Delta t \quad (3)$$

where $K_V(x,y,z)$ is the vertical eddy diffusivity field taken from the hydrodynamic model, K'_V is the first derivative of K_V with respect to the vertical coordinate z, and z_p is the vertical position of the particle. Following Ross & Sharples (2004), the local eddy diffusivity is calculated at $z_p^\star$ where

$$z_p^\star = z_p + \frac{1}{2}K'_V(z_p)\Delta t \quad (4)$$

The second term on the right hand side of Eq. (3) represents a displacement along the diffusive gradient. This adjustment to the simple random walk model is necessary to prevent artificial accumulation of particles in regions of low diffusivity (e.g. Hunter et al. 1993, Visser 1997, Ross & Sharples 2004).

Ross & Sharples (2004) have shown that in order to implement Eqs. (1) & (3) correctly, the time step of the random walk model must be substantially less than the second derivative of the diffusivity, i.e.

$$\Delta t < \mathrm{MIN}\left(\frac{1}{|K''_V|}\right) \quad (5)$$

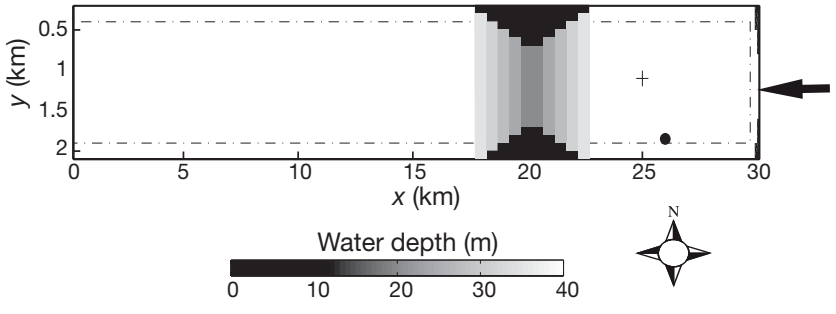

Fig. 1. Model domain and bathymetry. Inlet mouth is to the west ($x = 0$ km). Inlet depth is 40 m except in the sill region centred at $x = 20$ km, where depth shoals to 20 m. (●) Larval source. Velocity and salinity data shown in Fig. 2 are taken from the location marked by the cross. Arrow indicates where the river flow discharges into the inlet. Dash-dot line marks the inside edge of zone where coastal strip densities are calculated

The vertical diffusivity, K_V, can vary over the range $10^{-5} < K_V < 10^{-1}$ m^2 s^{-1} over short spatial scales. For this study, a time step for the random walk model of $\Delta t = 5$ s consistently satisfied the condition Eq. (5).

Louse behaviour and mortality. In Eq. (1), the vertical swimming speed $w_p(z)$ represents vertical migration and other aspects of louse behaviour that can be implemented through vertical particle motion. In the laboratory, copepodids prefer salinities >20 at 10°C (Johnson & Albright 1991), and avoid low surface salinities, aggregating at salinity discontinuities (Heuch 1995). The background swimming speed of *Lepeophtheirus salmonis* copepodids is reported by Heuch & Karlsen (1997) to be 1.55 mm s^{-1} (~5.5 m h^{-1}).

In the present model, 2 aspects of behaviour are invoked in addition to DVM: avoidance of low salinity, and avoidance of excessive depth. The latter is based on rather anecdotal evidence that salmon in 20 m deep pens are subject to less infestation by lice than salmon kept in 6 m deep pens (Huse & Holm 1993), suggesting lower copepodid abundance at depth (Heuch et al. 1995).

Initially, the vertical swimming speed is specified to simulate DVM, i.e.

$$w_p(z) = \begin{cases} -5.5 \text{ m h}^{-1} \text{ if } t_h < 6 \text{ or } t_h \geq 18 \\ +5.5 \text{ m h}^{-1} \text{ if } 6 \leq t_h < 18 \end{cases} \quad (6)$$

where t_h is the time of day in hours. But the values of $w_p(z)$ from Eq. (6) are overridden if the particle depth is >20 m, or the local salinity is <20, i.e.

$$w_p(z) = \begin{cases} +5.5 \text{ m h}^{-1} \text{ if } z_p > 20 \text{ m} \\ -5.5 \text{ m h}^{-1} \text{ if } S_p < 20 \end{cases} \quad (7)$$

where S_p is the local salinity at the particle location. Thus a larval particle is assumed to swim upwards if it finds itself (e.g. by vertical advection) at excessive depth, or to swim downwards to avoid excessively low surface salinities. Particles were not permitted to ground on the seabed or at the shoreline and these conditions, while enforcing $w_p(z) \neq 0$, led to particles accumulating at the surface in daylight and at 20 m depth at night. This accords with laboratory and field observations that copepodids, in particular, are positively phototaxic (Johannessen 1978), and aggregate in the surface waters during the day (Heuch et al. 1995, Penston et al. 2004). Behaviour patterns apply only to copepodids; nauplii are consistently modelled as passive particles, since their behaviour is thought to be much less pronounced than that of copepodids (Heuch et al. 1995) and quantitative data are not available.

Each model particle represented a cohort of sea louse larvae, and was assigned an 'abundance', N_t, which indicated the proportion of surviving larvae relative to the initial release. When a particle was released, $N_t = N_0 = 1$. Both nauplii and copepodids were made subject to natural mortality at a rate of 0.1 ind. d^{-1} (= 0.0042 h^{-1}), a rate typical for copepods (Hirst & Kiorboe 2002). Whereas copepodids were able to avoid harmful low salinity water (Heuch 1995), nauplii could not, and therefore suffered mortality when low salinities were encountered. For mortality of nauplii exposed to low salinity, we followed Brooks & Stucchi (2006) whereby water with salinity <30 had increasingly deleterious effects on survival as salinity reduced. N_t therefore evolved during the simulation according to

$$\frac{dN_t}{dt} = \begin{cases} -(a + \delta b)N_t & \text{if } S_p < 30 \\ -aN_t & \text{if } S_p \geq 30 \end{cases} \quad (8)$$

where a = 0.0042 h^{-1}, b = 0.4404 – (0.0148 × S_p) h^{-1}, and $\delta = 1$ when the larvae were nauplii, and $\delta = 0$ when the larvae were copepodids. The age of each particle, t_p, was used to monitor the stage development.

Experimental setup. The aim of this study was to investigate the effects of environmental conditions and larval behaviour on dispersal of sea louse larvae. To that effect, 4 simulations with varying freshwater discharge and an oscillating wind field were performed (Table 1). Each set of simulations was performed twice, both with and without larval behaviour patterns. For tides, we applied an oscillating water level with fixed amplitude of 1.5 m and a period of 12.4 h, typical of the dominant semi-diurnal M_2 tides in Scottish west coast waters. The latitude of the site was 57° N.

Simulations with low, medium and high freshwater discharge rates, Q_F, were performed. The different rates affected the salinity of the surface layer in the idealized fjord and the strength of the residual (non-tidal) circulation, which takes the form of a gravitational estuarine circulation. The runoff rates used were Q_F = 10, 50 and 200 m^3 s^{-1}.

An oscillating along-inlet wind was applied, with amplitude of 10 m s^{-1} and a period of 6 d. Wind forcing alternated between up-inlet and down-inlet directions lasting 3 d in each phase, allowing larvae to be transported in response to prolonged wind-

Table 1. Model of sea louse larvae dispersal experiments. Behaviour represents diel vertical migration, and depth and salinity avoidance by larvae

Run no.	River flow (m^3 s^{-1})	Wind	Behaviour
1	10	None	No
2	10	Oscillating	No
3	50	Oscillating	No
4	200	Oscillating	No
5	10	None	Yes
6	10	Oscillating	Yes
7	50	Oscillating	Yes
8	200	Oscillating	Yes

forcing events without invoking rather unrealistic steady wind conditions.

A source of larval sea lice was located in the inner basin of the inlet (Fig. 1), with coordinates $(x,y) = (26.0, 1.85)$. Larval particles were released continuously throughout the simulation, and were assigned an initial depth between 0 and 10 m, typical of salmon cage depths. A larval development rate appropriate for typical spring water temperatures (8 to 10°C) was simulated, with development time to the copepodid taking 5 d, and the copepodid stage lasting 7 d (Johnson & Albright 1991). The entire planktonic stage lasted 12 d and simulations were performed over a 24 d period to include 2 complete life cycles. Results were taken from the second half of the simulation, when the larval population was approximately stable with equal numbers hatching into and exiting from the larval stages. The results are normalized such that predicted abundance corresponded to a total egg hatch of 1 million eggs over the 12 d period. Abundance is presented in units of copepodids per model grid cell (each grid cell has a volume of 40 000 m^3).

RESULTS

Environmental forcing: salinity and velocity

The effects of the 4 variations of physical forcing on the salinity and velocity structure in the inner basin of the inlet are shown in Fig. 2. (Note that results from Runs 1 to 4 are shown, but that physical conditions for Runs 5 to 8 were identical). Profiles of mean along-inlet velocity over the 24 d simulation exhibit a classical fjordic estuarine circulation (Fig. 2a). At the surface, the mean flow is seaward, with a strength that is directly proportional to the river discharge. Beneath, the mid-depth flow is landward and also increases in strength with increasing runoff. The base of this layer at about 20 m depth coincides with the depth of the sill. Below 20 m, the mean flow is very weak in all cases as the deep water is isolated from the mean circulation by the sill.

Superimposed on the mean flow are fluctuations caused by tide and wind forcing. The oscillating along-inlet wind has a period of 6 d (Fig. 2b), and drives sur-

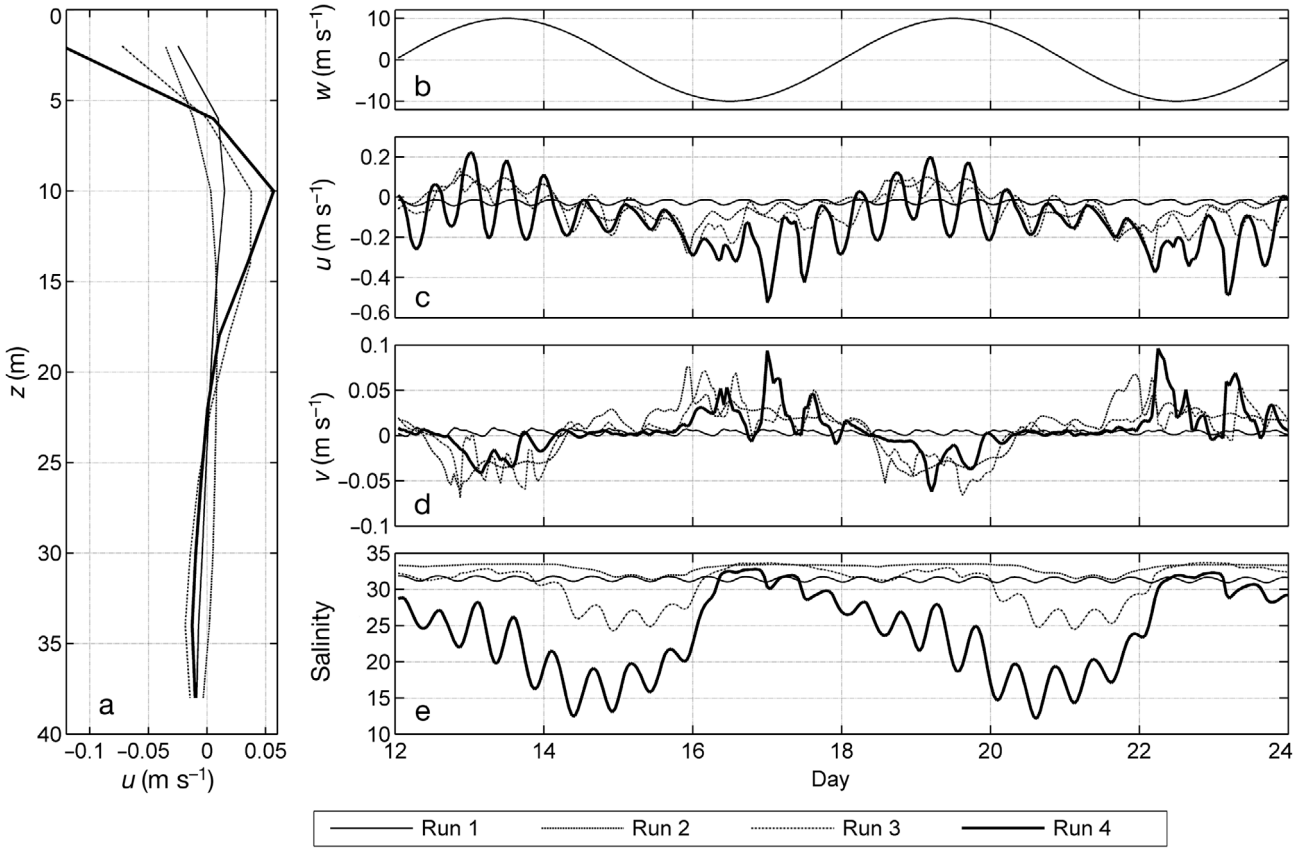

Fig. 2. Modelled velocity and salinity in the inner basin (see Fig. 1) for the 4 variations of physical forcing (Runs 1 to 4). (a) Vertical profiles of mean along-inlet velocity u, plotted against depth z. The velocities were averaged over the 12 d simulation. Time series of mean (b) along-inlet wind velocity w; (c) along-inlet surface layer velocity u; (d) across-inlet surface layer velocity v; and (e) surface layer salinity

face layer currents in Runs 2 to 4 (Fig. 2c). The strength of the wind-driven surface current increased with increasing river runoff and oscillated with the fluctuating wind forcing. Tidal currents in the inner basin were weak, and the surface flow on flood tides was only occasionally landward as the flood tide currents were generally not strong enough to overcome the surface layer outflow.

The influence of the Coriolis effect at the modelled latitude is seen in the across-inlet surface layer velocity (Fig. 2d). Along-inlet winds drive an across-inlet Ekman transport to the right of the wind direction, which fluctuated in direction as the wind switched from landward to seaward. In the simulation without wind (Run 1), there was a persistent, though weak, geostrophic flow towards the northern shore.

Surface layer salinity decreased with increasing river flow and fluctuated in response to wind and tidal forcing (Fig. 2e). Landward wind resulted in pooling of freshwater at the head of the inlet and lower salinities. Conversely, seaward winds push freshwater seaward, causing upwelling at the head of the inlet and increased salinity in the inner basin. Only during the simulations with the highest river flow (Runs 4 and 8) did surface salinities drop below 20, at which point sea lice avoidance strategies are invoked.

Copepodid dispersal and distribution

The infection risk to wild and farmed salmonids is posed by the infective copepodid, and the results presented here (summarised in Table 2) are therefore predicted copepodid distributions. Maximum predicted concentrations at each surface grid cell for simulations without larval behaviour (Runs 1 to 4) varied spatially by several orders of magnitude (Fig. 3). When wind stress was absent (Run 1), the highest abundance occurred in a relatively narrow band along the northern shore in the outer basin of the inlet (Fig. 3). The shoreline accumulation of infective larvae was caused by the across-inlet geostrophic surface current. When an oscillating along-inlet wind stress was introduced (Run 2), the alternating direction of the surface Ekman transport dispersed larvae across the inlet, reducing lateral variability in peak abundance (Fig. 3). As river flow increased (Run 3 and 4), greater numbers of copepodids were advected out of the inlet in the increasingly strong surface layer outflow, reducing peak abundance (Fig. 3). Consequently, the mean number of active copepodids within the model domain decreased as river flow increased (Table 2). With low runoff (Runs 1 and 2), typically 40% of hatched eggs survived to the infective stage and remained within the model domain, with the majority of the loss being due to natural mortality. Under medium and high runoff conditions, the proportion dropped to 8 and 2% respectively, as increased naupliar mortality due to lowered salinity and greater advective loss from the system were incurred. Advective loss was exacerbated as the water column stratified more strongly, because vertical diffusion was inhibited and, without active DVM, more larvae were retained in the increasingly strongly outflowing surface layer.

Introducing larval behaviour raised peak surface abundance, typically by an order of magnitude (Fig. 3, Runs 5 to 8). This was clearly a facet of DVM, with the synchronised movement of larvae to the surface elevating lice numbers there (see Fig. 4b). Wind forcing again enhanced copepodid dispersal horizontally and vertically, and increased river flow reduced the numbers of copepodids in the inlet (Fig. 3). In this instance, although the repeated entry of copepodids into the surface layer as a result of DVM subjected more individu-

Table 2. Sea louse larval dispersal simulations. Parameters are presented as temporal-mean values calculated over the 12 d simulation. All parameters, except salinity-related nauplius mortality (SRNM), refer to copepodids. M_1 and M_2 are the first and second moments of the distribution, respectively (Hunter et al. 1993). Surface layer, inlet head, and shoreline larval abundances are scaled for a hatch of 1 million eggs over 12 d. Larval behaviour is excluded in Runs 1 to 4 and included in Runs 5 to 8

Run	SRNM (%)	Surviving copepodids (%)	$M_1(x)$ (km)	$M_1(y)$ (km)	$M_1(z)$ (km)	$M_2(x)$ (km^2)	$M_2(y)$ (km^2)	$M_2(z)$ (km^2)	Surface layer abundance (lice cell^{-1})	Inlet head abundance (lice cell^{-1})	Shoreline abundance (lice cell^{-1})	Infected surface area (%)
1	0	38.8	11.0	0.5	14.0	16.4	0.1	51.5	1.0	0.0	100.8	7.7
2	0	40.8	14.6	1.0	16.3	31.1	0.3	92.4	4.6	1.3	39.9	36.1
3	11	8.8	13.4	1.0	14.4	51.2	0.3	76.6	0.8	2.4	10.3	10.9
4	30	2.0	15.5	1.1	12.3	58.2	0.3	59.6	0.2	2.6	2.2	3.4
5	0	43.5	13.4	0.5	9.9	10.4	0.1	3.1	19.4	0.0	108.7	16.9
6	0	38.6	16.7	1.0	10.8	44.7	0.2	31.3	13.4	1.2	53.5	34.4
7	11	13.4	17.4	1.2	10.3	75.8	0.3	24.8	5.1	15.3	20.1	26.9
8	31	4.8	17.1	1.2	9.8	61.2	0.3	15.6	1.9	2.0	5.9	18.2

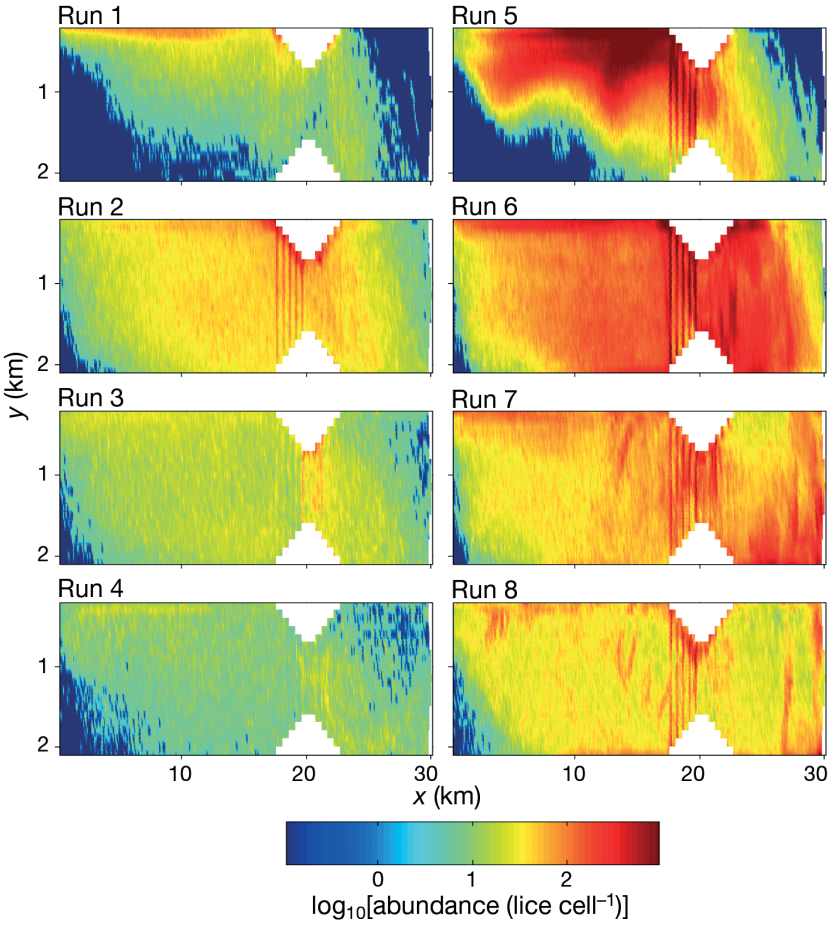

Fig. 3. Log values of maximum sea louse larval abundance predicted at each surface grid cell. The seaward end of the inlet is at $x = 0$ km. Panels show different model runs (Table 1); larval behaviour is excluded in Runs 1 to 4 and included in Runs 5 to 8. Abundance is plotted as $\log_{10}$(lice grid-cell^{-1}) and normalized for a hatch of 1 million eggs over 12 d. Note that the abundance in each cell is not necessarily contemporaneous. Due to the stepped nature of the model grid, higher abundance on the seaward slope of the sill (due to upwelling of larvae on the flood tide) is artificially banded

als to the surface outflow, the net loss from the system was less than in the cases without behaviour modelled.

The twice-daily fluctuations in $M_1(z)$ during Runs 1 to 4 (Fig. 4a) are due to tidal oscillations lifting and lowering the larvae, whereas the more pronounced oscillations during Runs 5 to 8 (Fig. 4b) arise from DVM which overrides tidal effects. The first (M_1) and second (M_2) moments of copepodid distributions represent, respectively, the location of the centre of mass and the variance of the population (Hunter et al. 1993), and are both calculated for each spatial dimension (x, y, z). The mean values of M_1 and M_2 over the simulation are presented in Table 2. Horizontal (x, y) dispersal increased with wind forcing and river flow, particularly along the inlet. Vertical (z) dispersal increased when wind forcing was included, but then decreased as runoff increased and the stronger stratification inhibited vertical mixing. The introduction of larval behaviour further increased horizontal dispersal, whereas vertical dispersal was reduced considerably (Table 2). Without behaviour, copepodids were evenly distributed throughout the water column (Fig. 4c), whereas inclusion of DVM produced 2 distinct peaks in the vertical distribution, one in the top 5 m, and a second at ~20 m depth (Fig. 4d).

Temporal variability and shoreline concentrations

The infection risk to wild salmonids depends not only on peak louse abundance, but also on the persistence of louse activity or 'occupation time'; i.e. the amount of time that copepodids are present in the surface layer (depth 0 to 4 m). The occupation time of copepodids varied widely, both spatially and between different simulations (Fig. 5). The spatial variation had similar features to the distributions of peak abundance (Fig. 3), suggesting that copepodids accumulated persistently in high numbers in the same locations within the inlet. For the low runoff simulations, DVM lowered the surface occupation time, relative to the cases without behaviour, since copepodids spent 50% of time at depth. As runoff increased, and active copepodid numbers fell, the occupation time also decreased and, in these cases, the higher numbers of surviving copepodids in Runs 7 and 8 relative to Runs 3 and 4 led to higher occupation times (Fig. 5).

Copepodid abundance at the inlet head (defined as a 200 m wide strip across the inlet at the landward end) (Fig. 6a,b) was highly variable, with abrupt peaks lasting about 6 to 18 h. Peak abundance was higher in the simulations with larval behaviour. In the simulations without wind, no larvae were predicted in the coastal strip at the head of the inlet. In the simulations with wind, larvae appeared at the head following periods of both up-inlet (e.g. Days 13 to 14) and down-inlet (e.g. Days 16 to 17) wind. In the former case, larvae were transported to the head of the inlet in the surface layer,

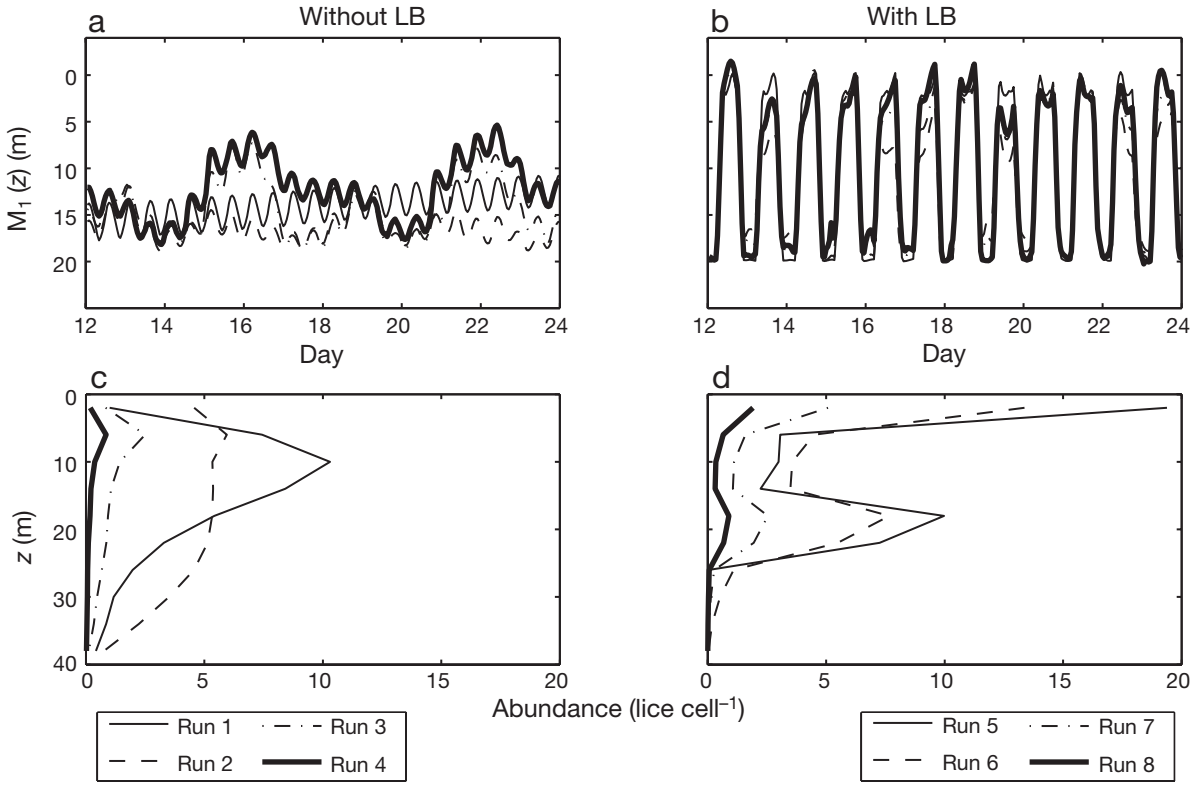

Fig. 4. Vertical location of sea louse copepodid population centre of mass, $M_1(z)$, (a) without and (b) with larval behaviour (LB). Predicted depth distribution of mean copepodid abundance (c) without and (d) with LB. Abundance (lice grid-cell^{-1}) is normalized for a hatch of 1 million eggs over a 12 d period

driven directly by the wind. In the latter case, larvae were transported in the deeper landward-flowing current which was strengthened by the seaward wind. In the simulations with behaviour, predicted copepodid abundance at the head was not higher than the mean for the whole surface layer (Table 2), except in the case of Run 7.

Copepodids located within a 200 m-wide coastal strip extending around the entire model coastline (Fig. 1) were counted to give 'shoreline' abundance (Fig. 6c,d). In this shoreline region, mean abundance over the simulation was markedly higher than the mean values for the whole surface layer (Table 2), and was higher when behaviour was included. Highest shoreline abundance occurred without wind forcing, when the persistent surface geostrophic flow concentrated larvae at the boundary. Fluctuations due to tide and DVM are apparent in the cases without and with larvae behaviour, respectively, but in both cases, these oscillations were obscured when wind forcing was included. Instead, abundance fluctuated at the frequency of the wind forcing, and also decreased with increasing river flow (Fig. 6c,d).

DISCUSSION

Our results show that, in coastal inlets with point sources of larvae (e.g. salmon farms), the dispersal and distribution of sea louse larvae are strongly influenced by environmental conditions and larval behaviour. Future models of sea louse dispersal must incorporate these physical and biological processes if predictions of infective louse distributions are to be used with confidence to assess the infection risk to farmed and wild salmonids. Our model simulates behaviour patterns specific to *Lepeophtheirus salmonis* but could easily be adapted for other louse species given appropriate data, and our fundamental conclusion remains the same: any form of behaviour involving vertical migration may affect larval dispersal and should be included in models.

Including larval behaviour in the dispersal model increased retention of larvae within the inlet and elevated predicted surface distributions relative to the passive particle simulations. Larval transport pathways were sensitive to the precise details of the interaction between the circulation and larval behaviour patterns.

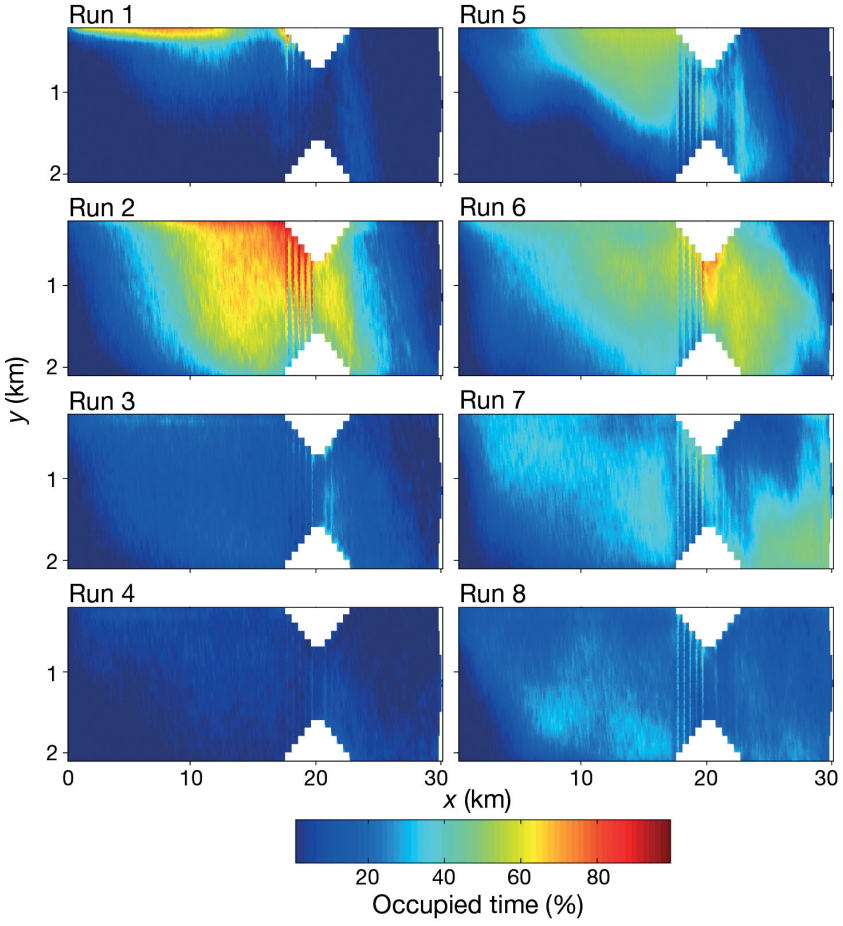

Fig. 5. Percentage of time during the 12 d simulation that surface layer model grid cells have at least one sea louse copepodid particle present. Panels show different model runs (Table 1); larval behaviour is excluded in Runs 1 to 4 and included in Runs 5 to 8. The seaward end of the inlet is at $x = 0$ km

For example, transport of copepodids to the head of the inlet was a combined function of wind forcing, runoff and larval behaviour, with transient peaks in copepodid abundance at the inlet head predicted during periods of both up-inlet and down-inlet wind. In the former case, larvae were transported to the head in the surface layer, whereas in the latter case transport took place in mid-water. In both cases, larvae reached the head of the inlet only when wind forcing strengthened the landward component of the circulation; transport by tidal currents alone was not sufficient to overcome the net seaward transport due to the estuarine circulation. Also, peaks only occurred at higher river flow rates ($Q = 50$ and 200 $m^3 s^{-1}$), when the landward flowing current at about 10 m depth (Fig. 1a) was strongest. It is interesting to note that, even with periodic wind forcing and constant river flow, the peaks in larval density at the inlet head were relatively short lived, lasting about 6 to 18 h (Fig. 6b). Under more variable wind forcing and river flow, the occurrence of larvae may be more sporadic still. The aggregation of copepodids in the surface layer and at depth due to DVM subjected more individual lice to the landward flowing current (whether at the surface or at depth), and thereby increased the predicted density of lice at the inlet head.

These model results concur with field observations that larval sea lice, primarily copepodids, are intermittently found in relatively high abundance in the shallow sub-littoral zone at the head of coastal inlets (Costelloe et al. 1998a,b, McKibben & Hay 2004). In Loch Shieldaig, the site of the study by McKibben & Hay (2004), the inlet tapers sharply towards the river mouth, which may exacerbate the aggregation of lice there. Costello (2006) suggested that louse larvae could be transported and concentrated into shallow estuarine waters by wind-driven currents; by aggregating at the surface or a halocline, there were increased chances of encountering salmonid hosts. The results shown here support Costello's hypothesis, and extend it by demonstrating that larvae can also be transported to the head of inlets at depth under seaward winds. Clearly, there are multiple potential transport pathways and conditions under which larval lice may be transported to the head of coastal inlets, which suggests that the infection risk to migrating salmonids leaving these rivers cannot be easily mitigated.

Predicted copepodid abundance throughout the inlet was also influenced by the prevailing environmental conditions. Under medium and high runoff conditions, mortality and advective loss from the system was high, lowering mean larval abundance. Larval behaviour reduced these losses, elevating mean surface layer abundance relative to the passive particle simulations. The wind-driven Ekman transport in the surface layer persistently trapped lice in high numbers against the northern shoreline, although the periodic landward wind partially dispersed these aggregations. Wide areas of the inlet were occupied by infective lice for more than 40% of the model simulation (except in the case of high river flow). This prediction of repeated aggregation of larvae in the same locations may be a facet of the idealized model bathymetry and periodic wind forcing used here. However, the existence of such zones of ele-

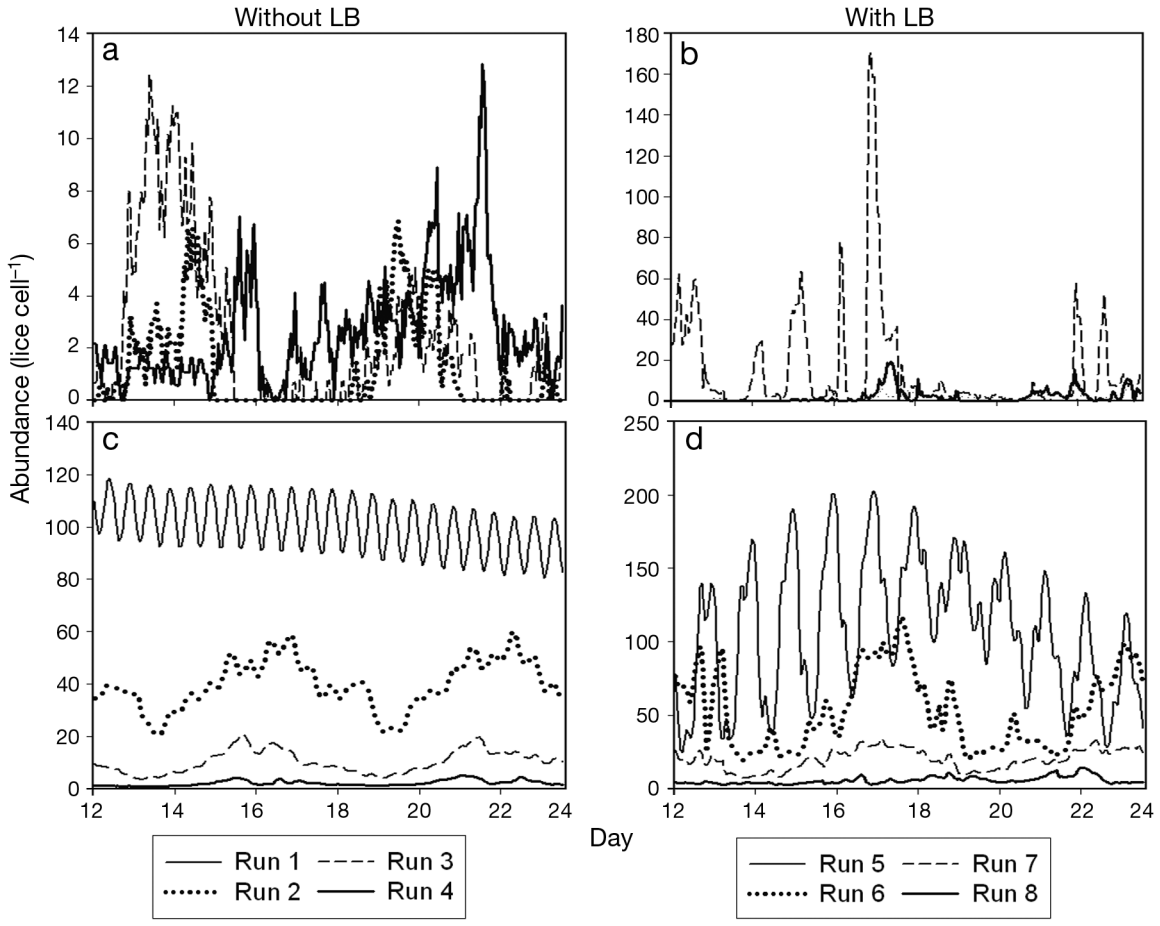

Fig. 6. Predicted sea louse copepodid abundance at the head of the inlet (a) without and (b) with larval behaviour (LB); and in the 200 m-wide shoreline strip around the inlet (c) without and (d) with LB. Abundance (lice grid-cell^{-1}) is normalized for a hatch of 1 million eggs over 12 d. Note different *y*-axis scales

vated copepodid abundance could explain why migrating salmonids in some coastal inlets are repeatedly subjected to high infection pressure. Sea louse infection of wild salmonids occurs soon after sea entry (Birkeland & Jacobsen 1997), and sea trout *Salmo trutta* in particular are very susceptible to sea lice because, unlike Atlantic salmon, the post-smolts remain in fjords and coastal areas close to their home river during the summer (Pemberton 1976, Berg & Berg 1987, Lyse et al. 1998). Post-smolts remain in surface waters close to or within the littoral zone, often in schools (Pemberton 1976, Lyse et al. 1998). In a Scottish sea loch, sea trout post-smolts initially remained within 200 m of the shore before moving out of the loch in summer (Pemberton 1976), and in a narrower Norwegian fjord, post-smolt sea trout generally remained within 10 m of the shore (Lyse et al. 1998). Our results suggest that it is these sub-littoral regions around the boundary of elongated inlets which may be particularly susceptible to elevated abundances of copepodids.

The dispersal of larvae predicted by each simulation is summarised by the moments, M_1 and M_2, of the distribution (Table 2). Note that the values of M_1, which represent the centre of mass of the population, are given relative to the origin of the model domain (at the northwest corner [Fig. 1]), with the larval source located at (x,y) = (26.0, 1.85) km. Increasing values of $M_1(x)$ thus indicate decreasing mean transport distances (of the population from its source) along the inlet. Our results demonstrate that larval behaviour (i.e. DVM) can reduce the mean distance that larvae are transported from the source, increasing retention within the inlet (Table 2). In every simulation, some copepodids reached the mouth of the inlet within their 12 d lifetime (Fig. 3), indicating that dispersal distances ranged over 26 km for all environmental conditions simulated here. Costello (2006) noted that dispersal of larvae may range from 5 to 17 km in low ambient currents to 23 to 70 km in stronger currents, with an average dispersal distance over 5 to 15 days of 27 km. Our results are of similar magnitude, though giving a

greater range under low current regimes, but because we do not track particles once they leave the model domain we are unable to better estimate dispersal distances in stronger currents. In a model of sea louse dispersal in the Broughton archipelago, where surface currents are strongly westward, Brooks (2005) predicted that louse larvae would travel 10 to 40 km within 5 d of release from fish farms in the region. That model did not include the effects of wind forcing, which may inhibit westward transport, and our results suggest that dispersal in the archipelago may have been overestimated if larvae migrated periodically into a deeper, landward-flowing layer and if that behaviour was not included in the model.

In another model of sea louse larval dispersal in the Broughton archipelago, Krkošek et al. (2005, 2006) fitted an advection-diffusion model to the distributions of sea louse larvae sampled from captured wild salmon. They observed and modelled local maxima in the distributions of both nauplii and infective copepodids within 0.5 km of fish farms in the region. In the present study, predicted peak abundances of nauplii consistently occurred close to the source (Fig. 7a), with secondary peaks occurring 5 km down inlet of the source. In contrast, the peaks in the mean distributions of copepodids occurred 7 to 12 km seaward of the source (Fig. 7b), as a result of net seaward transport during the development of larvae from hatching to copepodid stage. The individual daily along-inlet copepodid distributions predicted during Runs 7 and 8 (not shown) did, however, exhibit local maxima at the source location and at the head of the inlet on a number of occasions. These runs feature a strong estuarine circulation, which interacts with diurnal migration behaviour to enhance larval retention in the estuary and transport larvae in relatively high numbers into the inner region of the inlet. The high freshwater discharge into the Broughton Archipelago may similarly, and somewhat counter-intuitively, lead to enhanced retention of sea lice larvae if they can migrate into the deeper landward flowing layer, possibly explaining the observed peaks in copepodid densities close to fish farms (Krkošek et al. 2005). The contrasting modelling approach taken by Krkošek et al. (2005, 2006) with that of ourselves and Brooks (2005) offers an opportunity to gain further insights into how the interaction of physical and biological processes produces the observed distributions of larvae.

The behavioural parameters included in the model described here are based on very limited evidence taken from laboratory and enclosure studies. Further model development would benefit greatly from more quantitative data on larval (both copepodid and nauplii) swimming speeds, depth distributions, salinity tolerance and mortality rates. In addition, detailed field observations of larval sea louse behaviour in estuarine environments are essential to confirm the veracity of the laboratory data. The predictions are also fundamentally dependent on the underlying hydrodynamic model, which must accurately reproduce features of the circulation. In the present idealized study, the performance of the hydrodynamic model cannot be tested against data. However, in future applications to real environments, the hydrodynamic model must

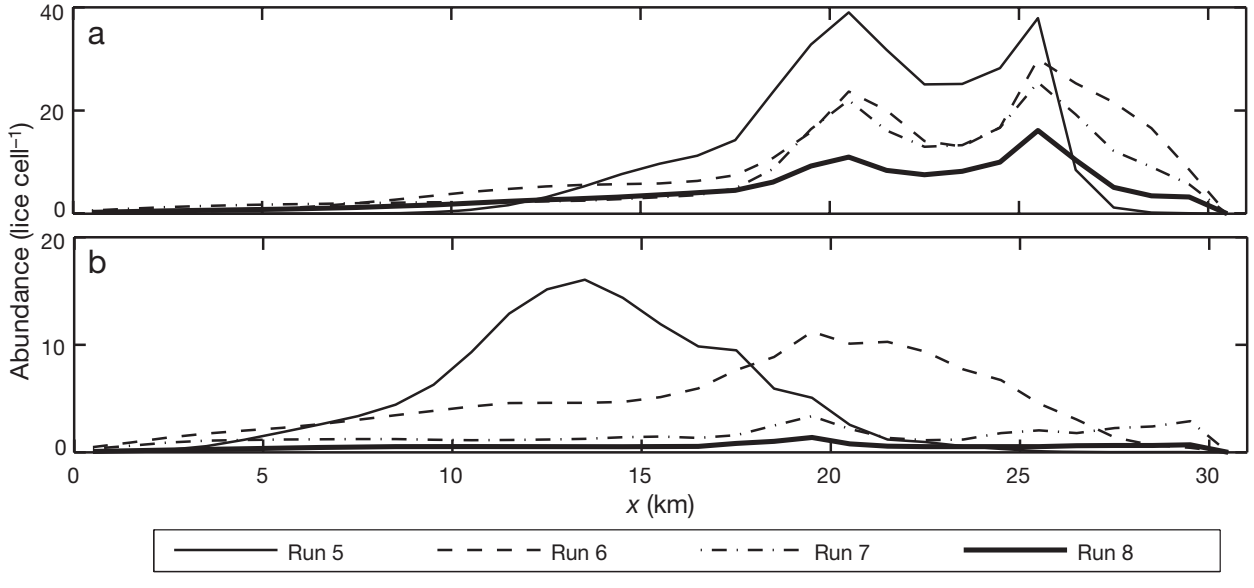

Fig. 7. Predicted mean abundance of (a) nauplii and (b) copepodids along the inlet from Runs 5 to 8. Abundance (lice grid-cell^{-1}) is normalized for a hatch of 1 million eggs over a 12 d period. Larval source: x = 26 km. Note different y-axis scales

resolve the vertical structure of the wind- and density-driven circulation, and the horizontal shape of the topography; e.g. small embayments where eddies may develop and act to retain larvae. We are in the process of modifying the louse transport model to run offline, so that the flow fields can be supplied by the most appropriate hydrodynamic model available.

Larval behaviour is complex, and models that depict sea lice as passively dispersing particles are over-simplistic and cannot be used as management tools with confidence. The results from this modelling study concur with field observations of sea louse distributions, which suggested that fish farms are a major source of sea lice in coastal inlets. Shoreline louse concentrations in a Scottish inlet correlated with farm production cycles and louse burdens (McKibben & Hay 2004), and sea louse infection levels on wild salmonids are often higher in intensive salmon farming areas (Tully et al. 1999, Bjorn et al. 2001). Coupled hydrodynamic–louse dispersion models that include key environmental and larval behavioural parameters will increase the confidence with which we can predict sea louse distributions and infection risk in coastal inlets, and so improve our ability to estimate the likelihood of transmission among salmon farms, and between farms and wild fish.

Acknowledgements. We thank A. Pike and 4 anonymous reviewers for comments that helped to improve this manuscript.

LITERATURE CITED

Asplin L, Boxaspen K, Sandvik AD (2004) Modelled distribution of salmon lice in a Norwegian fjord. ICES CM 2004/P:11

Berg OK, Berg M (1987) Migrations of sea trout *Salmo trutta* L., from the Vardnes river in Northern Norway. J Fish Biol 31:113–121

Birkeland K, Jacobsen P (1997) Salmon lice, *Lepeophtheirus salmonis*, infestation as a causal agent of premature return to rivers and estuaries by sea trout *Salmo trutta* L., post smolts. Environ Biol Fishes 49:129–137.

Bjorn PA, Finstad B (2002) Salmon lice *Lepeophtheirus salmonis* (Krøyer), infestation in sympatric population of Arctic Char, *Salvelinus alpinus* (L.), and sea trout, *Salmo trutta* (L.), in areas near and distant from salmon farms. ICES J Mar Sci 59:131–139

Bjorn PA, Finstad B, Kristoffersen R (2001) Salmon lice infection of wild sea trout and Arctic char in marine and freshwaters: the effects of salmon farms. Aquac Res 32:947–962

Brooks KM (2005) The effects of water temperature, salinity, and currents on the survival and distribution of the infective copepodid stage of sea lice (*Lepeophtheirus salmonis*) originating on Atlantic salmon farms in the Broughton Archipelago of British Columbia, Canada. Rev Fish Sci 13: 177–204

Brooks KM, Stucchi DJ (2006) The effects of water temperature, salinity and currents on the survival and distribution of the infective copepodid stage of the salmon louse (*Lepeophtheirus salmonis*) originating on Atlantic salmon farms in the Broughton Archipelago of British Columbia, Canada (Brooks, 2005) — a response to the rebuttal of Krkošek et al. (2005). Rev Fish Sci 14:13–23

Butler JA (2002) Wild salmonids and sea lice infestations on the west coast of Scotland: sources of infection and implications for the management of marine salmon farms. Pest Manag Sci 58:595–608

Costello MJ (2006) Ecology of sea lice parasitic on farmed and wild fish. Trends Parasitol 22:475–483

Costelloe M, Costelloe J, Coghlan N, O'Donohoe G, O'Connor B (1998a) Distribution of the larval stages of *Lepeophtheirus salmonis* in three bays on the west coast of Ireland. ICES J Mar Sci 55:181–187

Costelloe M, Costelloe J, O'Donohoe G, Coghlan NJ, Oonk, M, Van der Heijden Y (1998b) Planktonic distribution of sea lice larvae *Lepeophtheirus salmonis*, in Killary harbour, west coast of Ireland. J Mar Biol Assoc UK 78: 853–874

Gillibrand PA, Amundrud TL (2007) A numerical study of the tidal circulation and buoyancy effects in a Scottish fjord: Loch Torridon. J Geophys Res 112(C0):5030, doi:10.1029/2006JC003806

Heuch PA (1995) Experimental evidence for aggregation of salmon louse copepodids (*Lepeophtheirus salmonis*) in step salinity gradients. J Mar Biol Assoc UK 75:927–939

Heuch PA, Mo TA (2001) A model of salmon louse production in Norway: effects of increasing salmon production and public management measures. Dis Aquat Org 45:145–152

Heuch PA, Karlsen HE (1997) Detection of infrasonic water oscillations by copepodids of *Lepeophtheirus salmonis* (Copepoda: Caligida). J Plankton Res 19:735–747

Heuch PA, Parsons A, Boxaspen K (1995) Diel vertical migration: A possible host finding mechanism in salmon lice (*Lepeophtheirus salmonis*) copepodid? Can J Fish Aquat Sci 52:681–689

Hirst AG, Kiørboe T (2002) Mortality of marine planktonic copepods: global rates and patterns. Mar Ecol Prog Ser 230:195–209

Hunter JR, Craig PD, Phillips HE (1993) On the use of random walk models with spatially variable diffusivity. J Comput Phys 106:366–376

Huse I, Holm JC (1993) Vertical distribution of Atlantic salmon (*Salmo salar*) as a function of illumination. J Fish Biol 43(Suppl. A):147–156

ICES (2005) Report of the Working Group on North Atlantic Salmon (WGNAS), ICES CM 2005/ACFM:17, Nuuk, 5–14 April.

Johannessen A (1978) Early stages of *Lepeophtheirus salmonis* (Copepoda, Caligidae). Sarsia 63:169–176

Johnson SC, Albright LJ (1991) Development, growth and survival of *Lepeophtheirus salmonis* (Copepoda: Caligidae) under laboratory conditions. J Mar Biol Assoc UK 71: 425–436

Johnson SC, Treasurer JW, Bravo S, Nagasawa K, Kabata Z (2004) A review of the impact of parasitic copepods on marine aquaculture. Zool Studies 43:229–243

Krkošek M, Lewis MA, Volpe JP (2005) Transmission dynamics of parasitic sea lice from farm to wild salmon. Proc R Soc B 272:689–696, doi:10.1098/rspb.2004.3027

Krkošek M, Lewis MA, Morton A, Frazer LN, Volpe JP (2006) Epizootics of wild fish induced by farm fish. Proc Natl Acad Sci USA 103:15506–15510

Lyse AA, Stefansson SO, Ferno A (1998) Behaviour and diet of sea trout post-smolts in a Norwegian fjord system. J Fish Biol 52:923–936

McKibben MA, Hay DW (2004) Distributions of planktonic sea lice larvae *Lepeophtheirus salmonis* in the intertidal zone in Loch Torridon, Western Scotland in relation to salmon farm production cycles. Aquac Res 35:742–750

Murray AG, Gillibrand PA (2006) Modelling salmon lice dispersal in Loch Torridon, Scotland. Mar Pollut Bull 53: 128–135

Northcott SJ, Walker AF (1996) Farming salmon, saving sea trout: a cool look at a hot issue. In: Black KD (ed) Aquaculture and sea lochs. The Scottish Association for Marine Science, Oban, p 72–81

Pemberton R (1976) Sea trout in North Argyll sea lochs, population, distribution and movements. J Fish Biol 9:157–179

Penston MJ, McKibben MA, Hay DW, Gillibrand PA (2004) Observations on open-water densities of sea lice larvae in Loch Shieldaig, Western Scotland. Aquac Res 35: 793–805

Pike AW, Wadsworth SL (2000) Sealice on salmonids: their biology and control. Adv Parasitol 44:233–337

Ross ON, Sharples J (2004) Recipe for 1D Lagrangian particle tracking models in space-varying diffusivity. Limnol Oceanogr Methods 2:289–302

Saucier FJ, Roy F, Gilbert D, Pellerin P, Ritchie H (2003) Modelling the formation and circulation processes of water masses and sea ice in the Gulf of St. Lawrence, Canada. J Geophys Res 108(C8):3269, doi:10.1029/2000 JC000686

Simpson JH, Crawford WR, Rippeth TR, Campbell AR, Cheok JVS (1996) The vertical structure of turbulent dissipation in shelf seas. J Phys Oceanogr 26: 1579–1590

Tully O, Whelan KF (1993) Production of nauplii of *Lepeophtheirus salmonis* (Krøyer) (Copepoda: Caligidae) from farmed and wild salmon and its relation to infestation of wild sea trout (*Salmo trutta* L.) off the west coast of Ireland in 1991. Fish Res 17:187–200

Tully O, Gargan P, Poole WR, Whelan KF (1999) Spatial and temporal variation in the infestation of sea trout (*Salmo trutta* L.) by the caligid copepod *Lepeophtheirus salmonis* (Krøyer) in relation to sources of infection in Ireland. Parasitol 119:41–51

Visser AW (1997) Using random walk models to simulate the vertical distribution of particles in a turbulent water column. Mar Ecol Prog Ser 158:275–281

Editorial responsibility: Howard Browman (Associate Editor-in-Chief), Storebø, Norway

Submitted: March 31, 2007; Accepted: August 28, 2007
Proofs received from author(s): September 12, 2007